

This work was written as part of one of the author's official duties as an Employee of the United States Government and is therefore a work of the United States Government. In accordance with 17 U.S.C. 105, no copyright protection is available for such works under U.S. Law.

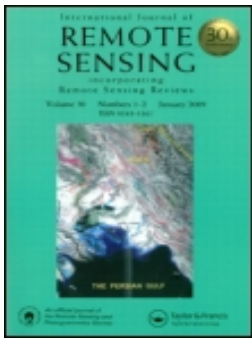
Public Domain Mark 1.0

<https://creativecommons.org/publicdomain/mark/1.0/>

Access to this work was provided by the University of Maryland, Baltimore County (UMBC) ScholarWorks@UMBC digital repository on the Maryland Shared Open Access (MD-SOAR) platform.

Please provide feedback

Please support the ScholarWorks@UMBC repository by emailing scholarworks-group@umbc.edu and telling us what having access to this work means to you and why it's important to you. Thank you.



Comparison of measurements and FluorMOD simulations for solar-induced chlorophyll fluorescence and reflectance of a corn crop under nitrogen treatments

E. M. Middleton , L. A. Corp & P. K. E. Campbell

To cite this article: E. M. Middleton , L. A. Corp & P. K. E. Campbell (2008) Comparison of measurements and FluorMOD simulations for solar-induced chlorophyll fluorescence and reflectance of a corn crop under nitrogen treatments, International Journal of Remote Sensing, 29:17-18, 5193-5213, DOI: [10.1080/01431160802036524](https://doi.org/10.1080/01431160802036524)

To link to this article: <https://doi.org/10.1080/01431160802036524>



Published online: 03 Dec 2010.



Submit your article to this journal [↗](#)



Article views: 433



View related articles [↗](#)



Citing articles: 1 View citing articles [↗](#)

Comparison of measurements and FluorMOD simulations for solar-induced chlorophyll fluorescence and reflectance of a corn crop under nitrogen treatments

E. M. MIDDLETON*[†], L. A. CORP[‡] and P. K. E. CAMPBELL^{†§}

[†]Hydrospheric and Biospheric Sciences Laboratory (Code 614.4), NASA/Goddard Space Flight Centre, Greenbelt, MD 20771, USA

[‡]Science Systems and Applications, Inc. (SSAI), Lanham, MD 20706, USA

[§]University of Maryland Baltimore Co. (UMBC), Catonsville, MD, USA

(Received 13 December 2006; in final form 4 December 2007)

Laboratory and field measurements previously acquired from foliage and canopies of corn (*Zea mays* L.) under controlled nitrogen (N) fertilization were used to parameterize and evaluate a new spectral vegetation Fluorescence Model (FluorMOD) developed to include the effects of steady-state solar-induced chlorophyll fluorescence (SIF) on canopy reflectance. These data included biophysical properties, fluorescence (F) and reflectance spectra for leaves; reflectance spectra of canopies and soil; solar irradiance; plot-level leaf area index (LAI); and canopy SIF emissions determined using the Fraunhofer line-depth (FLD) principle for the atmospheric telluric oxygen absorption features at 688 nm ($O_2\beta$) and 760 nm ($O_2\alpha$). FluorMOD simulations implemented in the default mode did not reproduce the observed magnitudes of leaf F, canopy SIF, or canopy reflectance. However, simulations for all of these parameters agreed with observations when the default FluorMOD information was replaced with measurements, although N treatment responses were underestimated. The observed shift in the red/far-red SIF ratio (from <1 to ~ 2) that occurred in scaling from leaves to canopies, partially attributed to the paucity of abaxial leaf information incorporated in the model, was not expressed in the simulations. Recommendations were provided to enhance the potential utility of FluorMOD in support of SIF field experiments and studies of agriculture and ecosystems.

1. Introduction

Solar-induced chlorophyll fluorescence (SIF) from vegetation canopies is indicative of plant physiological function and allows early detection of environmentally induced stress. However, the relationship between steady-state fluorescence (F) produced at the leaf level and the signal detected at the top of the canopy, or above the atmosphere by remote sensing techniques, is very complex. Therefore, models have been developed since the early 1990s to better quantify the relationships affecting the top-of-canopy F by consideration of factors influencing F measurements from single leaves. The work of Rosema *et al.* (1998) led to the development of the FLSAIL model, an extension of the SAIL (Scattering by Arbitrarily Inclined Leaves) model (Verhoef 1984, 1998) that included canopy architecture parameters. The FluorMOD canopy F model (Petrós *et al.* 2005) builds on these earlier efforts.

*Corresponding author. Email: Elizabeth.M.Middleton@nasa.gov

It includes the dependence of F emissions on the photosynthetically active radiation (PAR) conditions (Verhoef 2005), especially as influenced by leaf orientation with respect to the Sun's position and changes in light quality with depth inside the canopy for the incident downward and diffuse upward fluxes.

An objective of the FLuorescence EXplorer (FLEX) mission (Moreno 2005), a concept under development through the European Space Agency (ESA), is to use FluorMOD for simulating realistic SIF above vegetation surfaces and to estimate its detection from space. The FLEX mission concept relies on retrieval of steady-state SIF from the apparent vegetation canopy reflectance spectra using the Fraunhofer line-depth (FLD) principle (Plascyk 1975), for two major atmospheric telluric oxygen absorption features: $O_2\beta$, centred at 688 nm; and $O_2\alpha$, centred at 760 nm. SIF varies with vegetation status (species, phenology, vigour, etc.) and can be linearly dependent on PAR illumination intensity (as shown by Liu *et al.* 2005). The intensities of SIF expected from vegetation across landscapes have yet to be fully characterized, and a consensus has not yet been reached on the optimal methods for SIF measurements or their expected SIF magnitudes. Currently, estimates made with different instruments and species under different conditions vary for canopy red SIF from 1.5 to $10.5 \text{ mW m}^{-2} \text{ nm}^{-1} \text{ sr}^{-1}$, while canopy far-red SIF estimates range from 0.5 to $12.0 \text{ mW m}^{-2} \text{ nm}^{-1} \text{ sr}^{-1}$ (Theisen 2000, Campbell *et al.* 2002, Moya *et al.* 2003, 2004, Dobrowski *et al.* 2005, Liu *et al.* 2005, Louis *et al.* 2005, Corp *et al.* 2006a,b, Meroni and Colombo 2006, Guanter *et al.* 2007).

This range in values could be attributed to several factors, including: large variations in the illumination conditions during data acquisitions; the differing species, growth stages and associated canopy architectures; a range of SIF responses to different environmentally induced plant stressors; differing SIF retrieval methods; and/or uncertainties in the units of measurement.

Our research group has been investigating several aspects of F properties of foliage and canopies, including SIF. Using the FLD principle applied to spectra spanning the two oxygen bands, we estimated canopy average red (at 688 nm) SIF values of $4.3 \pm 1.0 \text{ mW m}^{-2} \text{ nm}^{-1} \text{ sr}^{-1}$ and far-red (at 760 nm) SIF values of $2.0 \pm 0.8 \text{ mW m}^{-2} \text{ nm}^{-1} \text{ sr}^{-1}$ for a cornfield, under a PAR intensity of $1660 \mu\text{mol m}^{-2} \text{ s}^{-1}$ using an Analytical Spectral Devices (ASD) FieldSpec FR spectroradiometer (Middleton *et al.* 2006, Corp *et al.* 2008). Further justification for using ground-based ASD measurements over a cornfield to provide estimates of chlorophyll fluorescence (ChlF) is supported by a recently published study (Guanter *et al.* 2007). The authors found that ground-based ChlF measurements made with the ASD correlated strongly with narrow-band ($<2.2 \text{ nm}$) estimates acquired over crops from the Compact Airborne Spectrographic Imager (CASI)-1500 sensor, from which the far-red SIF was $\leq 5 \text{ mW m}^{-2} \text{ nm}^{-1} \text{ sr}^{-1}$. Our previous *in situ* corn canopy SIF levels, which fall within the range suggested by other investigations (including Guanter *et al.* 2007), were used in the present study along with contemporaneously acquired supporting field and laboratory measurements for a rigorous preliminary evaluation of FluorMOD. The plausibility of using actively induced F information gained from laboratory measurements on individual leaves for estimating the SIF that occurs in nature under ambient illumination and other environmental conditions for vegetation canopies, through scaling-up methods based on one-dimensional (1-D) radiative transfer models, is addressed.

2. Materials and methods

2.1 Plant material, field and leaf measurements

A corn (*Zea mays* L.) crop was arranged in plots within three complete blocks at the United States Department of Agriculture (USDA) in Beltsville, MD, USA. Each plot received a controlled nitrogen (N) fertilization regime at one of four dosages (280, 140, 70 and 0 kg N/ha) in experiments conducted in August 2004. These treatments augmented existing soil N levels by 200, 100, 50 or 0% of the recommended rate. Measurements were made when the crop had achieved the grain-filling reproductive (R3) growth stage and had attained a height of ~ 3 m. Leaf-level measurements were obtained from the 13th leaf (the ear leaf) and included optical properties (reflectance, transmittance and absorptance), chlorophyll content (using procedures described in Wellburn 1994), specific leaf mass and other physiological measurements (Middleton *et al.* 2006). Plot-level leaf area index (LAI) was measured contemporaneously using the Li-Cor 2000 (Li-Cor, Lincoln, NE, USA).

The canopy spectra were acquired using an ASD-FR FieldSpec Pro spectroradiometer (Analytical Spectral Devices, Inc., Boulder, CO, USA). This spectroradiometer uses a 512-channel array of silicon photodiodes overlaid with an order separation filter to provide a 3-nm full-width at half-maximum (FWHM) spectral resolution, sampled at 1.4 nm. Nadir radiances were measured at 1 m above plant canopies (4 m above the soil surface) with an ASD within a 22° field of view, providing a ~ 1.2 m ground resolution. A second ASD radiometer simultaneously acquired solar irradiance spectra over a stationary Spectralon reference panel (Labsphere, North Sutton, NH, USA). Canopy ASD measurements were obtained on a clear day at noon ± 2 hours (photosynthetic photon flux density $\sim 1660 \mu\text{mol m}^{-2} \text{s}^{-1}$). Nadir canopy spectral reflectance was calculated as the ratio of canopy radiance to panel irradiance for each sample, and presented as percentage reflectance per waveband.

2.2 Laboratory fluorescence measurements

Actively induced F spectra were obtained in the laboratory for both adaxial and abaxial surfaces at selected discrete excitation (EX) wavelengths, including 420 nm (420EX) and 532 nm (532EX), using a Fluorolog-II spectrofluorometer (Spex Industries, Edison, NJ, USA). EX spectra were also obtained for emissions at the peak ChlF wavelengths, F680 and F740. For the adaxial leaf surfaces, excitation–emission matrices (EEMs) were produced at a spectral resolution of ≤ 5 nm, for EX wavelengths between 400 and 750 nm and emission (EM) wavelengths between 600 and 800 nm. A standard, calibrated EEM was constructed from these measurements on leaves from each N treatment, and values near the F peaks were interpolated (referred to below as the standard, solar uncorrected EEM). A solar-corrected EEM was developed from the standard EEM by applying correction factors to achieve a spectral profile and intensity for the xenon illumination source, which closely resembled that of the solar spectrum, as determined from mid-day summer irradiance spectra collected with an ASD over a Spectralon panel (Campbell *et al.* 2008) for PAR at $1660 \mu\text{mol m}^{-2} \text{s}^{-1}$. Simulated adaxial leaf SIF intensities ($\text{mW m}^{-2} \text{nm}^{-1} \text{sr}^{-1}$) were then obtained through integration of monochromatically acquired EX spectra (Corp *et al.* 2006b). Other details on the instrumentation and methodologies for F measurements can be found in Corp *et al.* (2006b, 2008) and Middleton *et al.* (2005, 2006).

Direct determination of leaf-level SIF was also independently achieved on these samples. In the laboratory, leaves were individually provided with a simulated full solar spectrum from a 250 W solar simulator (Oriel 91160A, Newport Stratford Inc., Stratford, CT, USA) outfitted with a Global Air Mass Filter (Oriel 81080, Newport Stratford Inc.) and an ASD spectrometer. The system simulated mid-day solar irradiation typical for the Washington, DC (USA) area in mid-July and was used to illuminate leaves held in special frames. These measurements were acquired for leaf areas of $\sim 2 \text{ cm}^2$ using an ASD spectroradiometer with a sensor foreoptic view angle of 8° , with a Spectralon panel serving as a reference. To determine the ChlF contribution, a Schott RG 665 long-pass filter was used to prevent F induction by wavelengths below 665 nm. Before illumination, leaves were dark-adapted for 5 min, and steady-state ChlF (as a stable minimum F that was thereafter maintained for 1 min) was achieved ~ 30 s after illumination, as described in Campbell *et al.* (2002, 2008). This method was used to separately induce and measure foliar ChlF, in addition to apparent foliar spectral reflectance (ChlF plus reflected radiation) across the 650–800 nm region, for the adaxial surfaces of the 2004 leaves (Campbell *et al.* 2007) and for both adaxial and abaxial surfaces of leaves examined in a previous 2001 field experiment (Campbell *et al.* 2002).

2.3 FLD determination of SIF over the cornfield

SIF was extracted from the apparent canopy reflectance spectra at 688 and 760 nm using the FLD principle (Plascyk 1975, Zarco-Tejada *et al.* 2000, 2004b, Corp *et al.* 2006b). The FWHM for these two major telluric features is 4 nm for $\text{O}_2\beta$ (centred at 688 nm) and 7 nm for $\text{O}_2\alpha$ (centred at 760 nm). The following algebraic expressions of the FLD principle adapted from Plascyk (1975) were used to obtain canopy reflectance (R) and SIF from vegetated surfaces in each of these bands:

$$\text{Reflectance, } R = (c - d)/(a - b), \quad (1)$$

$$\text{Fluorescence, as SIF} = d - Rb = (ad - cb)/(a - b), \quad (2)$$

where a and b represent the reference panel radiances, within and outside each O_2 feature, respectively; c and d represent the comparable target radiances. This method was applied to the above-canopy ASD upwelling and downwelling spectra acquired at marked locations with the N plots; the irradiance spectra were normalized to $1660 \mu\text{mol m}^{-2} \text{ s}^{-1}$ because SIF is correlated with PAR intensity (Liu *et al.* 2005), to enable comparison across N treatments acquired throughout the mid-day period. At the time of this 2004 field experiment, we were uncertain whether the spectral resolution of the ASD was sufficient for the quantification of SIF within these major telluric O_2 features. The ASD spectroradiometers use a 512-channel silicon photodiode array overlaid with an order separation filter to provide a 3 nm FWHM spectral resolution at a 1.4 nm sampling resolution. This resolution does allow extraction of F information within the major telluric O_2 features from apparent reflectance. However, the accuracy of retrievals using the FLD method is uncertain because the 3 nm bandwidth may include the shoulder spectral regions on either side of the absorption feature, a condition that would elevate the retrieval estimate. Consequently, determinations made in the future with higher spectral resolution should provide estimates with greater accuracy and precision.

2.4 FluorMOD

The FluorMOD combines plant F, leaf and canopy radiative transfer equations, and a simple forward scattering atmospheric model for top-of-atmosphere radiances, to predict the spectral responses of vegetation, including SIF. The FluorMOD V3.1 graphic user interface (Zarco-Tejada *et al.* 2004a) was used to link the inputs and outputs from both FluorMODleaf and FluorSAIL modules to provide realistic top-of-canopy SIF. Leaf input parameters include total chlorophyll ($a+b$), water equivalent thickness, dry matter content, F quantum efficiency, leaf temperature, species temperature dependence, and stoichiometry of Photosystem II (PSII) to Photosystem I (PSI) reaction centres, in addition to soil reflectance and solar irradiance. Other inputs of the model describe the canopy architecture, given by the LAI, two leaf inclination distribution function parameters and the hotspot parameter, the illumination and viewing geometries, and two parameters describing the dependence of leaf F on the PAR intensity.

The output from FluorMODleaf is passed to FluorSAIL, for which output parameters include the solar irradiance, sky irradiance, total irradiance, radiance without F, radiance with F included, total radiance, reference reflectance, total reflectance, reflectance (from SAIL), the ratio SAIL/FluorSAIL, and reference and total top-of-atmosphere radiances (the latter was not corrected for atmospheric variability due to aerosols and water vapour, etc.). Initially, we generated FluorSAIL canopy outputs based on FluorMODleaf look-up table information, in conjunction with measured vegetation parameters summarized in table 1, to simulate leaf reflectance and F spectral properties (the ‘default’ mode). Subsequently, the FluorSAIL canopy component of the model was run using our measurements for vegetation parameters, leaf and field spectra, and upward EEMs for the adaxial foliar surfaces (referred to below as the ‘revised’ mode). Unfortunately, we did not have measured downward EEMs of the abaxial surfaces to replace the ‘default’ downwelling matrices in FluorMOD.

3. Results and discussion

The 2004 biophysical data used here for the FluorMOD parameterization/ comparison are summarized in table 1. A full description of the leaf, canopy and crop measurements acquired in two growing seasons (2004, 2005) at the USDA cornfield appears elsewhere (Middleton *et al.* 2005, 2006, Corp *et al.* 2006a, 2008).

Table 1. N Treatment effects on biophysical measures of field corn growth.

Treatment* (%)	Chl _{ab} ($\mu\text{g cm}^{-2}$)	$C_m \times 10^{-3}$ (g DW cm^{-2})	C_w (m)	LAI
200	67 a†	6.4 a	1.65 a	3.14 a
100	62 b	6.2 a	1.63 a	2.74 a
50	57 c	5.9 b	1.60 b	2.45 b
0	34 d	5.6 c	1.57 b	2.05 c

Chl_{ab}, total chlorophyll; C_m , specific leaf area; C_w , leaf water content; and DW, dry weight.

*N treatment levels are expressed as a percentage of the recommended rate (140 kg N/ha).

†Column-wise mean values represent corn growth parameters at the R3 (grain fill) development stage. Means with the same letter were not separable by ANOVA_{LSD,05}.

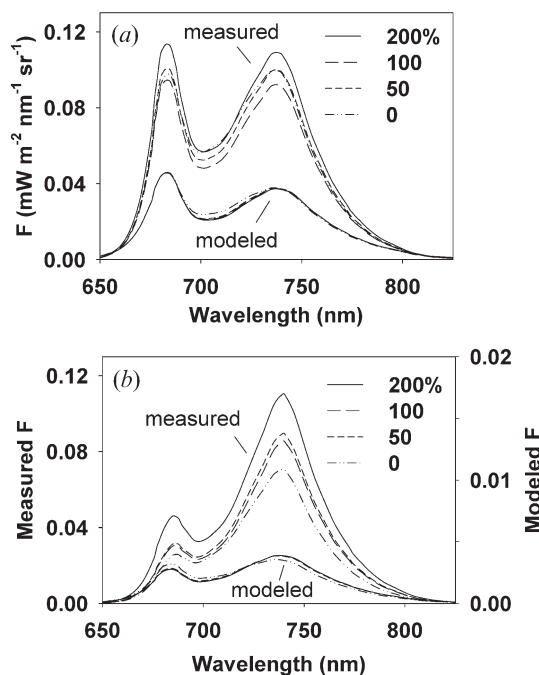


Figure 1. Emission spectra. Measured versus modelled ChlF emission spectra (650–850 nm) are grouped separately, for F ($\text{mW m}^{-2} \text{nm}^{-1} \text{sr}^{-1}$) of the adaxial surfaces of corn leaves from four N treatments (0, 50, 100 and 200% of optimal N, shown with different line types). Emission spectra are for two excitation wavelengths: (a) 420 nm (420EX), where both the measured and modelled spectra share the same 'y' axis, and (b) 532 nm (532EX), where the measured and modelled spectra have different axes (measured on left, modelled on right). Measured spectra were solar corrected.

3.1 Leaf chlorophyll fluorescence

A comparison of ChlF EM spectra (650–850 nm) of corn leaves obtained from measurements versus estimates from FluorMOD (figure 1) reveals that the model simulations produced much lower F values than the measurements at two selected EX wavelengths (420EX, 532EX). Model underestimates were approximately one-third that of measured values for emissions produced with 420EX, and more than an order of magnitude lower for those produced with 532EX (figure 1(a) vs. 1(b)). For the 420EX case, the relative magnitudes of the red and far-red ChlF peaks were about equal, as expressed in both the measured and simulated spectra (figure 1(a)). However, for 532EX, the measured far-red ChlF peaks were 2–3 times greater than the red peaks, but they were approximately equal in the simulated spectra (figure 1(b)). For measured emissions, the far-red ChlF peaks were similar (~ 0.07 – $0.11 \text{ mW m}^{-2} \text{nm}^{-1} \text{sr}^{-1}$) from both EX wavelengths, although N treatments were better captured with 532EX (figure 1(a) and 1(b)). These ChlF values appear small because they represent emissions resulting from sequential monochromatic wavelength EX.

In the EX spectra (figure 2), as for the EM spectra above, N treatment differences were well expressed in the leaf-level F measurements but were not apparent in the simulations. As was obtained for the EM spectra, underestimates also occurred in EX spectra for the simulated emissions at the ChlF peaks (680 and 740 nm) when

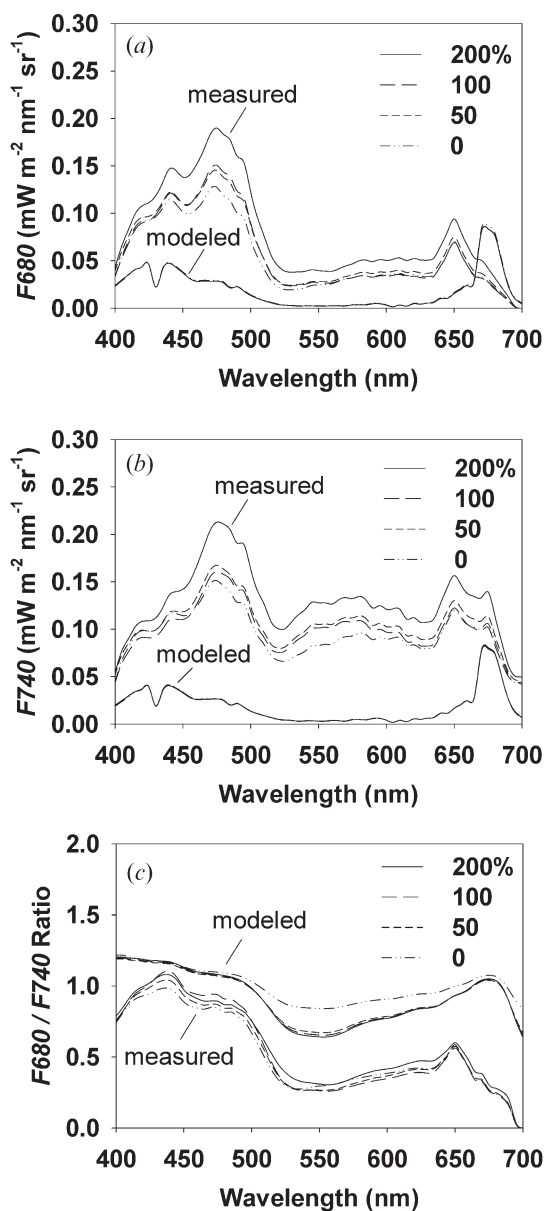


Figure 2. Excitation (EX) spectra. Measured versus modelled ChlF EX spectra (400–800 nm) for the ChlF peaks produced by the adaxial surfaces of corn leaves from N plots: (a) red ChlF emissions at 680 nm; (b) far-red ChlF emissions at 740 nm; and (c) the red/far-red ChlF emission ratio, F680/F740. The measured and modelled spectra are grouped (as indicated) and measured spectra were solar corrected. Within each group, N treatments (0, 50, 100 and 200% of optimal N) are shown with different line types. Fluorescence intensities are given in $\text{mW m}^{-2} \text{nm}^{-1} \text{sr}^{-1}$.

compared to the measured, solar-corrected (normalized to measured solar irradiance) ChlF.

There appears to be a shift in the modelled red ChlF (F680) resulting from blue excitation, with peaks produced at 420 and 440 nm instead of 430 and 470 nm as

observed in the measured EX spectra, and as would be expected to match established chlorophyll *b* and carotene absorption features (figure 2(a)). The underestimate of the simulated far-red ChlF (F740) emissions as a function of EX wavelength is much greater, and especially deficient throughout the green region (figure 2(b)). Furthermore, it appears that the same EX curves were used to create these F680 and F740 responses (e.g. note the feature at 675 nm in figures 2(a) and 2(b)).

The red/far-red emission ratio (F680/F740) was determined from the information given in figures 2(a) and 2(b) (see also figure 2(c)). The excitation spectra produced for this F680/F740 ratio by FluorMOD show values close to 1.0 ($\sim 20\%$) except for a $\sim 40\%$ decrease centred at ~ 530 nm (figure 2(c)). However, this ratio should fall to zero beyond 680 nm in concert with F680 emissions, as observed in the measured ratio spectra (figure 2(c)). The measured F680/F740 ratio spectra exhibit a similar but more pronounced shape, with most values of the ratio falling well below 1.0 and with a $\sim 70\%$ decrease centred at ~ 530 nm (figure 2(c)), beyond which the measured F680/F740 ratios are ≤ 0.6 at green to red EX wavelengths.

One reason for the FluorMOD underestimates of corn leaf F is shown in the 3-D EEM plots (figure 3), where the solar-corrected EEM (normalized to solar irradiance, figure 3(a)) was compared with the EEM created from FluorMOD (figure 3(b)). The correction for the total solar PAR intensity of $1660 \mu\text{mol m}^{-2} \text{s}^{-1}$ and for the actual spectral variations in intensity across the visible (VIS, 400–700 nm) solar irradiance spectrum, relative to the flat irradiance spectrum of the lamp source, enhanced F intensities, especially in the green region (~ 500 – 600 nm), where solar irradiance is higher relative to the far-red region. The standard EEM (not shown) is similar to figure 3(a).

The relative difference between the solar-corrected versus the FluorMOD EEM for the 200% N group, presented as a 2-D contour plot (figure 4(a)), indicates that the greatest discrepancies ($\leq 0.12 \text{ mW m}^{-2} \text{ nm}^{-1} \text{ sr}^{-1}$) occurred for far-red ChlF emissions across most EX wavelengths. The impact of performing the solar correction on the standard EEM is highlighted for the 200% N group (figure 4(b)); here, the subtle differences between the solar-corrected and standard EEMs are apparent, whereas they are difficult to see in a 3-D plot. Figure 4(b) shows that solar correction augmented ChlF (especially in the peaks) emanating from blue EX wavelengths; the far-red ChlF emissions were also augmented when produced from green EX wavelengths; reductions in F occurred for the ChlF peaks when they resulted from longer wavelength EX (> 650 nm) or EX < 430 nm. The impact of the experimental range of N treatments (0–200%) on the solar-corrected, measured EEMs is shown for a similar 2-D difference plot group (figure 4(c)), as F for the high (200% N) group minus F for the lowest (0%) N. The greatest differences ($\leq 0.02 \text{ mW m}^{-2} \text{ nm}^{-1} \text{ sr}^{-1}$) due to N availability occurred in both the red and far-red ChlF peaks resulting from EX centred around ~ 470 nm, and for far-red ChlF from green (~ 550 nm) EX wavelengths.

3.2 Leaf-level SIF

Figure 2(a,b) shows that F680 emanated largely from excitation by the blue and green wavelengths, whereas F740 resulted from contributions that were more distributed across the VIS EX spectrum. This is shown more clearly by the stacked, coloured bars in figure 5(a,b), where the ChlF peak emissions were solar-corrected and integrated across EX wavelengths in the VIS spectrum to obtain estimates of

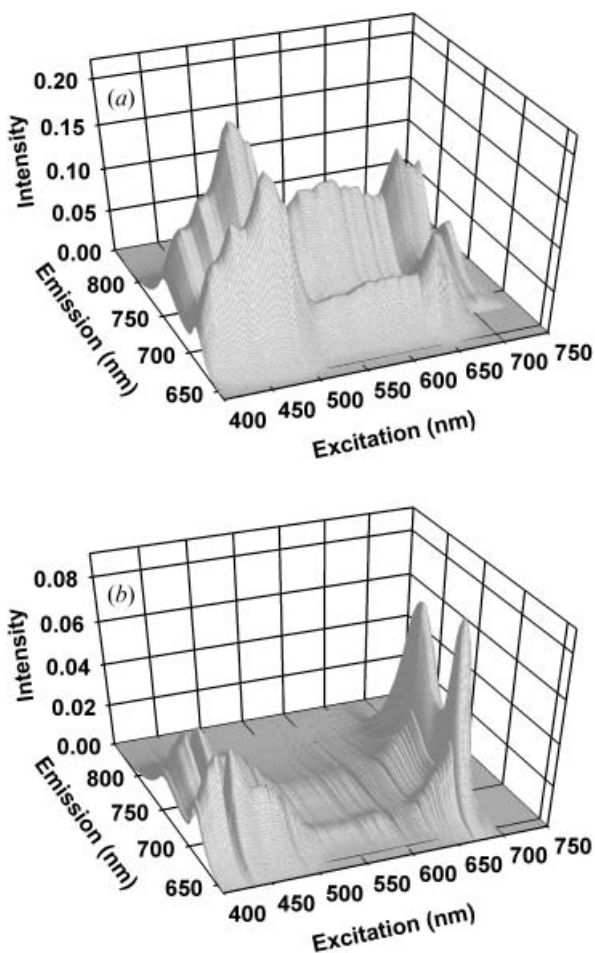


Figure 3. Leaf-level 3-D plots for measured versus modelled fluorescence EEMs of adaxial surfaces of corn leaves provided high N (200%) expressed as a function of PAR illumination intensity of $1660 \mu\text{mol m}^{-2} \text{s}^{-1}$; (a) the measured, calibrated and solar-corrected EEM; and (b) the FluorMOD simulated EEM, which assumes a spectrally flat illumination source. Fluorescence intensities (z axis) are given in $\text{mW m}^{-2} \text{nm}^{-1} \text{sr}^{-1}$ (note the different scales for (a) vs. (b)). The x and y axes are emission (nm) and excitation wavelengths (nm), respectively. EEMs were produced at a spectral resolution of 5 nm.

leaf adaxial SIF resulting from polychromatic EX, as occurs in natural ambient solar environments. From this fluorometric method, it can be estimated that approximately two-thirds of F685, but only 30–40% of F740, was elicited by wavelengths below 600 nm. For corn data acquired in the 2004 field season, red and far-red SIF for the 200%N group were 4.7 and $8.2 \text{ mW m}^{-2} \text{nm}^{-1} \text{sr}^{-1}$, respectively (figure 5(a) vs. 5(b)). These were significantly greater (by $\sim 2 \text{ mW m}^{-2} \text{nm}^{-1} \text{sr}^{-1}$) than for the lower N treatments (0–100%).

Leaf SIF estimated with a second, independent method using hyperspectral reflectance observations and simultaneous polychromatic (rather than sequential monochromatic) induction from a solar simulator (figure 5(a,b) open bars) produced slightly lower (by $\sim 1\text{--}2 \text{ mW m}^{-2} \text{nm}^{-1} \text{sr}^{-1}$) red and far-red SIF values but similar treatment differences, as compared to those derived with fluorometry. As we

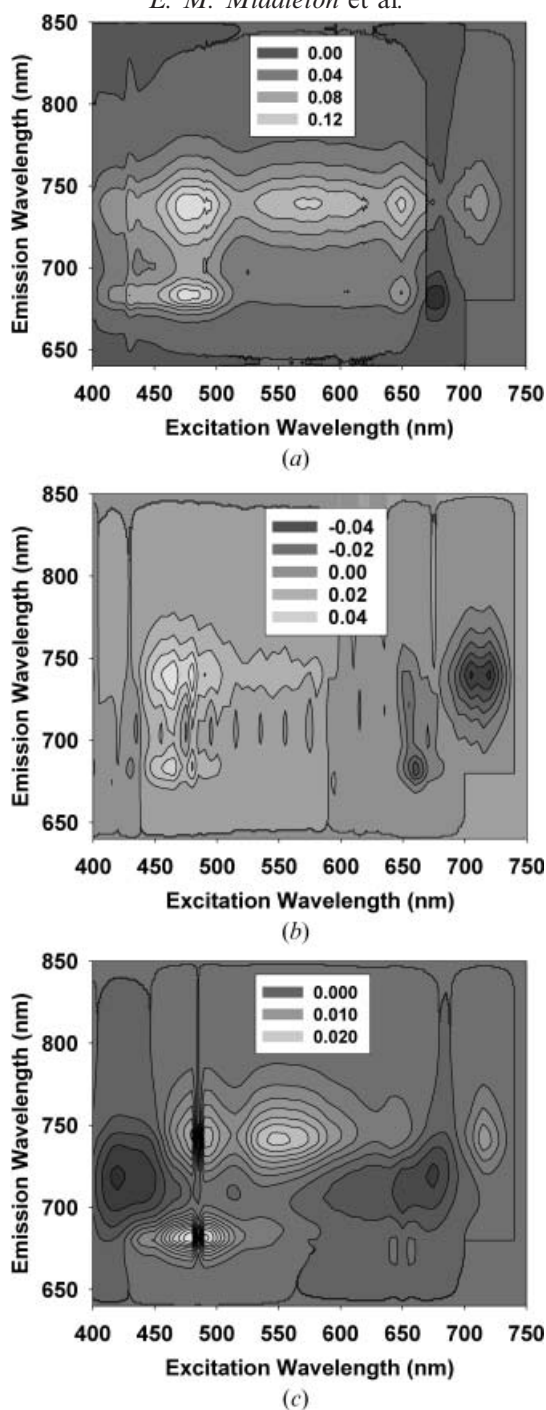


Figure 4. Leaf-level 2-D contour difference plots for measured versus modelled fluorescence EEMs of adaxial surfaces of corn leaves: (a) the difference plot for the measured, solar-corrected EEM – FluorMOD EEM, for high N (200%); (b) the difference plot for the measured, solar-corrected EEM – standard uncorrected EEM, also for high N (200%); and (c) the difference plot for the measured, solar-corrected EEMs, high N (200%) – low N (0%). Fluorescence intensity differences are presented in 3–5 categories ranging from 0 to $0.12 \text{ mW m}^{-2} \text{ nm}^{-1} \text{ sr}^{-1}$.

demonstrated earlier that far-red SIF is especially sensitive to differences in the relative weighting of illumination wavelengths (figure 4), the differences in spectral quality between the light sources for the SPEX vs. the solar simulator probably contribute to this result. In addition, the lamp PAR intensity of the solar simulator

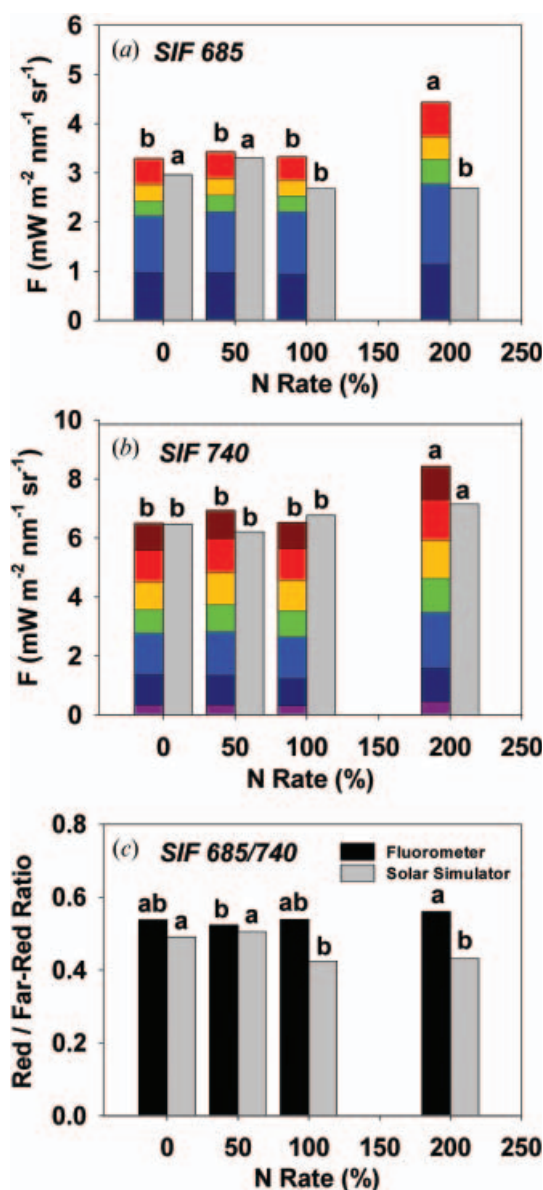


Figure 5. Calculated (a) red (680 nm), (b) far-red (740 nm) and (c) red/far-red SIF emissions resulting from active excitation of the adaxial surfaces of corn leaves in the laboratory from four N treatment levels. F intensity is shown for seven spectral excitation regions: UV (300–400 nm), blue (400–450 nm), blue-green (450–500 nm), green (500–550 nm), yellow (550–600 nm), orange (600–650 nm) and red (650–700 nm) wavelengths. Calculations are based on solar-corrected EEMs, with F intensities expressed in $\text{mW m}^{-2} \text{nm}^{-1} \text{sr}^{-1}$. Grey bars are for a solar simulator, otherwise, bars are for fluorometer measurements. Bars with the same letter are not separable by $\text{ANOVA}_{\text{LSD},0.05}$.

($\sim 1275 \mu\text{mol m}^{-2} \text{s}^{-1}$) was lower than the ambient solar level used for standard comparisons ($1660 \mu\text{mol m}^{-2} \text{s}^{-1}$) with the fluorometer method. Nevertheless, the F685/F740 ratios produced by the two independent methods for these samples were very similar ($\sim 0.57 \pm 0.14$, figure 5(c)) across N treatments.

Data obtained from corn leaves in 2001 using this second method to derive SIF from leaf reflectances of both adaxial and abaxial surfaces are shown in

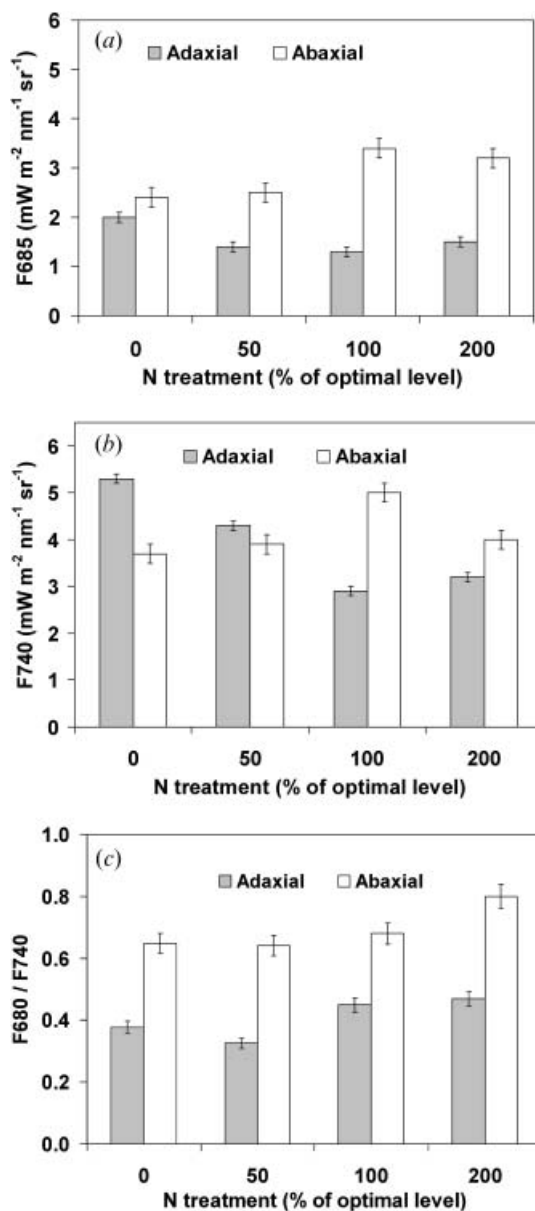


Figure 6. The leaf-level SIF produced in the laboratory at the ChlF peaks, 685 and 740 nm, is shown for both adaxial (filled) and abaxial (unfilled) leaf surfaces of corn leaves, for four N treatment levels: (a) F685; (b) F740; and (c) the F685/F740 SIF ratio. SIF intensities are expressed in $\text{mW m}^{-2} \text{nm}^{-1} \text{sr}^{-1}$. The illumination source was a solar simulator, and measurements were made with an ASD spectroradiometer.

figure 6(a–c). The effect of N treatments in that year and site differ from the trend captured in the 2004 data. Here, adaxial SIF estimates were lower than those obtained in 2004 (figure 5 vs. figure 6) for the 200% N treatment group: F685 (figure 5(a)), $\sim 2.7 \pm 0.2 \text{ mW m}^{-2} \text{ nm}^{-1} \text{ sr}^{-1}$; F740 (figure 5(b)), $\sim 7.1 \pm 0.2 \text{ mW m}^{-2} \text{ nm}^{-1} \text{ sr}^{-1}$; and F685/F740 ratio, 0.43 ± 0.01 (figure 5(c)). Similar trends were reported, but somewhat lower values were obtained, with an ASD for two C_3 crops (sunflower and tobacco) by Alonso *et al.* (2007). The most impressive new information is that F685 from the leaf undersides (the abaxial surfaces) was significantly larger than for adaxial surfaces for all N groups. For example, the 200% N group produced abaxial F685 and F740 of 3.2 ± 0.1 and $4.1 \pm 0.2 \text{ mW m}^{-2} \text{ nm}^{-1} \text{ sr}^{-1}$, respectively (figure 6(a,b)). F740 was greater for abaxial surfaces only in the higher (100% and 200%) N treatments. However, the F685/F740 ratio for abaxial surfaces was substantially larger ($0.6\text{--}0.8 \pm 0.2$) across all N treatments relative to comparable values for their upper surfaces ($0.3\text{--}0.5$, figure 6(c)). These results indicate that N effects on corn differ year to year, and that abaxial surfaces may potentially impact canopy SIF when under physiological stress.

3.3 Canopy SIF

The leaf-level SIF characterizations were used to estimate canopy SIF emissions with FluorMOD (figure 7). The modelled canopy SIF was very low ($< 1 \text{ mW m}^{-2} \text{ nm}^{-1} \text{ sr}^{-1}$) when executed in the ‘default’ mode, and did not express N treatment effects. After replacing the default FluorMOD information with our own measurements for leaf and environmental spectra, including solar-corrected SIF (i.e. the ‘revised’ mode), the simulated canopy SIF was enhanced by a factor of ~ 5 , the far-red SIF peak exceeded the red peak intensity, in agreement with leaf-level observations, and N treatment effects on SIF were captured (figure 7).

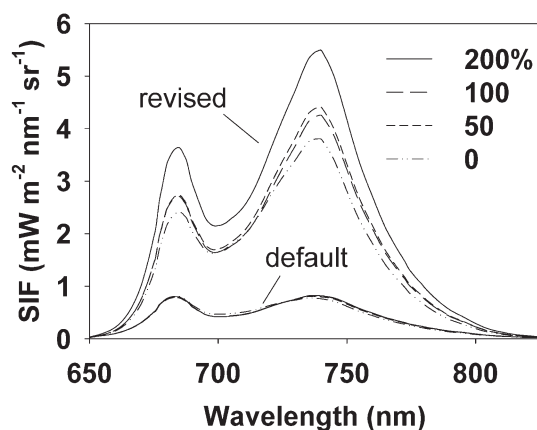


Figure 7. Canopy/crop simulations for SIF from FluorMOD using either the ‘default’ FluorMOD information or SIF ‘revised’ information obtained by replacing or supplementing the default information with our field measurements. The revised FluorMOD SIF simulations incorporated our measured leaf reflectance and transmittance spectra, in addition to field measurements for solar irradiance, soil reflectance, the biophysical input parameters listed in table 1, and our solar-corrected upward fluorescence matrices. The default FluorMOD downward fluorescence matrices were retained because measurements were not available. Within each group, N treatments (20, 50, 100 and 200% of optimal N) are shown with different line types. Fluorescence intensities are expressed in $\text{mW m}^{-2} \text{ nm}^{-1} \text{ sr}^{-1}$.

When the FluorMOD simulation was run in this adaptive, revised mode, canopy SIF at the red and far-red ChlF peaks was ~ 3.4 and $\sim 5.6 \text{ mW m}^{-2} \text{ nm}^{-1} \text{ sr}^{-1}$, respectively, for the high (200%) N group. These simulated values for the canopy (figure 7) are somewhat lower than for individual leaves (figure 5(a,b)) because they represent the integrated influences of non-photosynthetic material, including the soil/litter background. However, relative N treatment effects agree with leaf-level trends. In addition, the estimated red/far-red SIF ratio (F688/F760) changed from ~ 0.95 in 'default' simulations to 0.61 in 'revised' simulations, consistent with the leaf-level values presented above. Consequently, replacing the 'default' leaf spectra and EEMs with measurements greatly enhanced and improved characterization of the corn canopy SIF responses, as estimated from either laboratory method to estimate leaf SIF (fluorometry, reflectance). However, we might have achieved a better correspondence to measured canopy SIF (by producing higher red canopy SIF), as discussed below, if we had been able to provide abaxial EEMs for the 'revised' FluorMOD simulations. It should be noted that diurnal changes in leaf and canopy SIF have not been addressed in these examinations, although mid-day reductions in ChlF and/or SIF have been reported (Dobrowski *et al.* 2005, Louis *et al.* 2005).

In the revised mode, FluorMOD's estimate of canopy SIF for F688 in the 200% N group ($3.7 \text{ mW m}^{-2} \text{ nm}^{-1} \text{ sr}^{-1}$) was only slightly lower than our *in situ* field SIF values for F688 ($4.3 \pm 1.0 \text{ mW m}^{-2} \text{ nm}^{-1} \text{ sr}^{-1}$), but the comparable SIF for F760 was more than twice as high as our field values (5.6 vs. $2.0 \pm 0.8 \text{ mW m}^{-2} \text{ nm}^{-1} \text{ sr}^{-1}$). Although both the 'default' and 'revised' FluorMOD simulations indicate a canopy red/far-red SIF ratio (F688/F760) ≤ 1.0 (figure 7), we obtained values > 1.0 in our ASD field determinations of this ratio (Corp *et al.* 2008): ~ 1.4 for the higher (100% and 200%) N groups and 3.9 for the lower two (0% and 50%) groups. Consequently, a closer agreement between model vs. field estimates was achieved only for the most vigorous 'unstressed' vegetation, as expected, because FluorMOD does not specifically address vegetation responses to environmental treatments.

The discrepancy between canopy SIF observed in the field and SIF estimates generated from leaf-level adaxial laboratory F information might be partially explained by the higher ChlF emissions of abaxial leaf surfaces that influence canopy SIF, responses that are also not sufficiently described in FluorMOD. Where red SIF is 2–3 times greater for abaxial than adaxial surfaces of healthy, vigorous vegetation (as shown in figure 6), and subject to multiple scattering within the canopy, the resulting canopy red SIF would be enhanced over leaf-level values. A red/far-red ratio > 1.0 has also been reported by other researchers (e.g. Campbell *et al.* 2002, 2008, Liu *et al.* 2005, Meroni and Colombo 2006). It is also highly likely that the field retrievals with the ASD, while providing useful preliminary estimates, include a bias and a variance that might be resolved or reduced with higher spectral resolution and refinements to the FLD algorithm. A recent study (Guanter *et al.* 2007) successfully retrieved ChlF from $\text{O}_2\alpha$ using both ground-based ASD and CASI aircraft spectroradiometers having $\sim 3 \text{ nm}$ resolution. Continued efforts by our research team are being directed towards this goal with a spectrometer having approximately 1 nm resolution, to obtain simultaneous *in situ* high-resolution reflectance and laser-induced fluorescence observations from plant canopies (Corp *et al.* 2003, 2008).

3.4 Leaf-level reflectance

At the leaf level (figure 8), FluorMOD simulations produced reflectance spectra that generally agreed with measured spectra. These spectra show apparent leaf

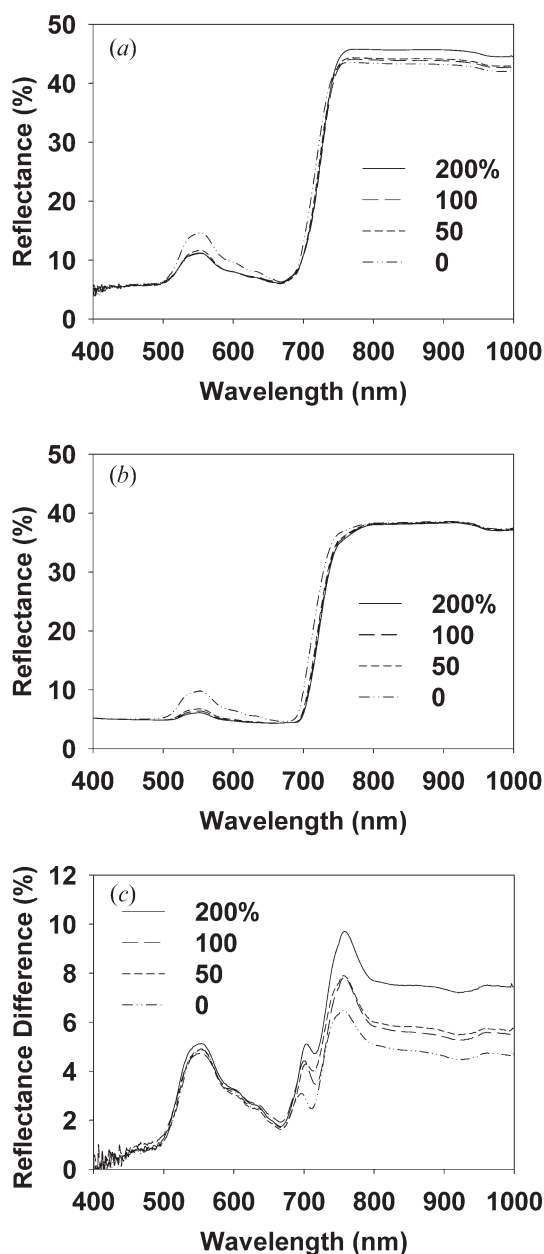


Figure 8. Leaf-level reflectance spectra (400–1000 nm). Measured versus simulated ‘apparent reflectance’ (reflectance plus fluorescence) spectra (400–1000 nm) for adaxial surfaces of corn leaves from N plots: (a) measured with an ASD spectroradiometer and an integrating sphere; (b) simulated with FluorMOD in the ‘revised’ mode, using measured leaf characteristics (see table 1) with measured leaf and field spectra; and (c) the difference spectra (observed – simulated, (a) – (b)). Within each group, N treatments (0, 50, 100 and 200% of optimal N) are shown with different line types. Reflectance is given as a percentage (of reference illumination).

reflectance (reflectance+SIF). In both measured (figure 8(a)) and modelled (figure 8(b)) leaf spectra, the 0% N treatment produced a higher green reflectance than other groups, although the model simulations underestimated the measured value (10% vs. 15%). In the near-infrared region (NIR, 800–1000 nm), the 200% N treatment generated a higher measured reflectance (at ~46%, figure 8(a)) than other N treatments, but the FluorMOD reflectances were lower (at ~37%, figure 8(b)) and did not exhibit N treatment effects.

The difference spectra (observed minus modelled, figure 8(c)) indicate that reflectance was underestimated at all wavelengths (450–1000 nm) in the model simulations. There were no N treatment effects in the VIS region, where measurements were up to 5% higher than FluorMOD estimates (with the greatest difference at 560 nm). However, discrepancies between FluorMOD and measured spectra were most apparent in the NIR region, where differences increased with N treatments (0–200%) and the largest (6–10%) occurred at 760 nm, the location of the O₂ α feature. A small shift in the red edge for modelled vs. measured leaf spectra was also expressed in the difference spectra near 700 nm.

3.5 Canopy reflectance

Much better correspondence was achieved between FluorMOD simulations and canopy measurements for apparent canopy reflectance spectra (figure 9) than for canopy SIF. FluorMOD simulations made in the 'revised' mode with our spectral measurements produced good correspondence to ASD field reflectance measurements (figure 9(a,b)), especially for the 0% N group. However, canopy reflectance was underestimated by a few per cent in the other N groups (e.g. -1.5% at 570 nm, 50–200% N; -6% at 930 nm, for 200% N). Both the measured and FluorMOD canopy spectra expressed additional responses to N deficiency, captured in the greater blue-ward shift of the red edge and lower NIR coupled with enhanced green reflectance. Further examination of the red edge demonstrates that N treatment effects were more pronounced in the measured canopy spectra. For example, an 8 nm shift (738 to 730 nm, high to low N treatment) was observed in the measured canopy red edge, whereas only a 4 nm shift (733 to 729 nm) was seen in modelled canopy spectra.

The measured ASD canopy reflectance spectra were lower in intensity than measured leaf spectra (figure 9(a) vs. figure 8(a)), but exhibited greater N treatment effects in the green and NIR regions. For example, canopy reflectance in the green (at 570 nm) was 5–7%, compared with leaf reflectance of 11–15%; canopy NIR reflectance ranged between 27% and 42%, compared with leaf reflectance of 43–46%. One notable feature of the measured canopy spectra, not reproduced in FluorMOD simulations, was an increase in reflectance from the NIR shoulder (~760 nm, 0% N; ~770 nm, 200% N) that reached maximum values at 930 nm. These effects could be due to a combination of several factors, including: the influence of exposed soil and dead leaves in the lower parts of canopies (especially in the 0% and 50% N treatments); representation of the canopy as a single homogeneous layer composed of adaxial leaf surfaces by FluorMOD; differences in leaf display in response to N treatment that affected the projected LAI of adaxial vs. abaxial leaf surfaces; and differences in leaf morphology throughout the vertical canopy profile that were not captured in the measurements of each plants' representative (#13) leaf or in FluorMOD canopy characterizations.

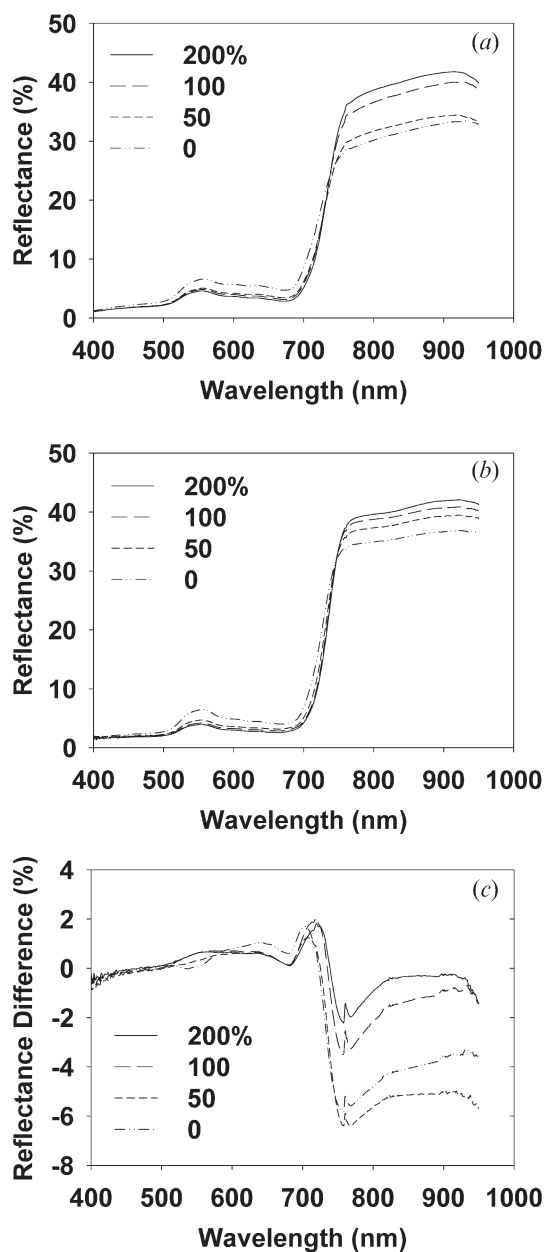


Figure 9. Canopy/crop spectra (400–1000 nm). Measured versus simulated canopy/crop ‘apparent reflectance’ (reflectance plus fluorescence) for corn N plots: (a) measured with a spectroradiometer 1 m above the corn canopy; (b) simulated with FluorMOD using leaf and field spectral inputs (the ‘revised’ mode); and (c) the difference spectra (observed – simulated, (a) – (b)). Within each group, N treatments (0, 50, 100 and 200% of optimal N) are shown with different line types. Reflectance is given as a percentage (of reference illumination).

The canopy apparent reflectance difference spectra (figure 9(c)) revealed that FluorMOD estimates agreed with measurements in the VIS region ($\sim 2\%$). However, FluorMOD overestimated (by $\sim 3.5\%$) the NIR reflectance of the two high N treatments, especially around the 760 nm feature ($O_2\alpha$). FluorMOD overestimates

were greater ($\sim 6.5\%$) for the two low N treatments. Separation of the high and low N groups in the difference spectra occurred at about 710 nm. A small spike at 760 nm indicates some residual differences for modelled and measured SIF.

In general, FluorMOD modelled the canopy reflectance for the high N 'unstressed' treatments fairly successfully. This indicates that the FluorMOD default information based on the physiology and morphology of C_3 bean leaves is more relevant to the conditions associated with the thicker, healthy corn leaves than the thinner, N-deficient C_4 monocot leaves, and perhaps the proportion of standing green/brown vegetation in the canopy. In the two low (0% and 50%) N groups, canopies were up to 0.25 m shorter and their lower one-third to one-half portions were composed entirely of dead, attached leaves at the time of measurements. By contrast, the thicker, larger and wider leaves of the high (100% and 200%) N groups produced more ChlF and had larger scattering and absorbing surfaces in a taller canopy. Evidently, more information (e.g. total LAI) is needed to supplement green LAI in describing the canopy foliage density and distribution for stressed vegetation.

4. Conclusions

In this study we conducted an evaluation of the performance of FluorMOD by using field and laboratory measurements of reflectance, F, and biophysical properties of corn leaves and corn plots under N fertilization regimes. We pursued this endeavour despite uncertainties introduced by using different instruments and methods associated with estimating leaf-level SIF from actively induced, monochromatic data and with uncertainties associated with the application of the FLD approach to field data acquired with an ASD spectroradiometer.

We found that FluorMOD, when provided measurements specific to the vegetation to be modelled, produced canopy SIF simulations that were close to 'reality' for our cornfield under N treatments, especially for red SIF (e.g. F688). The agreement (within $1 \text{ mW m}^{-2} \text{ nm}^{-1} \text{ sr}^{-1}$) of red SIF from FluorMOD with values retrieved in the field from ASD reflectance spectra strengthens our confidence in the application of the FLD for this band. However, far-red canopy SIF (e.g. F760) was overestimated in simulations, as far-red > red SIF in revised FluorMOD runs, whereas $F760 < F688$ in the field. We are confident that the ASD field estimate of F760 provides a useful preliminary SIF determination. Thus, the ability to capture leaf to canopy shifts in the red/far-red SIF ratio, probably associated with the arrangement of foliar material in 3-D space, has not been demonstrated in these FluorMOD simulations. Inclusion of high-quality abaxial matrices may improve future simulations.

The satisfactory correspondence between the canopy-level FluorMOD simulations and the ASD canopy spectra was accomplished by substituting FluorMOD's leaf-level 'default' characterizations with measured information. We did not obtain useful F estimates with FluorMOD by using the 'default' look-up table information plus our biophysical measurements (table 1). In that mode, serious shortcomings were revealed in the fundamental leaf-level characterizations of the FluorMOD fluorescence matrices, which produced underestimates for steady-state ChlF and apparent reflectance that were subsequently manifested as underestimated steady-state SIF and apparent reflectance at the canopy level. Consequently, our study highlights the importance of verifying the integrity of F spectra (e.g. EEMs), then correcting or normalizing them with solar irradiance information, in order to

estimate SIF at the leaf and canopy scales. This correction ensures that excitation across the solar irradiance wavelengths, especially in the green spectrum, adequately represents true contributions to SIF. This has an important impact on the far-red ChlF emissions and consequently on the red/far-red SIF ratio.

Currently, FluorMOD does not include spectral reflectance or F information specific to corn (a C₄ species), nor does it specifically address spectral responses to environmental stress such as drought, nutrient deficiencies, high light and high/low temperature exposures, or the influence of SIF from leaf undersides. We suggest that future upgrades to FluorMOD might consider replacing existing default EEMs with new leaf-level matrices displaying corrected spectral characteristics; normalizing these leaf-level EEMS using measured solar irradiance to obtain ambient SIF; adding the capability to simulate spectral responses to environmental stresses, including influences on leaf display that affect the projected distribution of foliage within canopies (e.g. projected adaxial/abaxial leaf surface ratio); adding more species types, including corn; augmenting the user documentation; and providing prototype data assemblage sets (EEMS, leaf spectra, etc.) for the vegetation expected to be examined in upcoming field campaigns.

In addition, it is hoped that field SIF experiments will be comprehensive, to include extensive laboratory F measurements in support of field spectral observations, coupled with biophysical and physiological measurements of vegetation. Our intention is to assist the remote sensing and F community to improve SIF characterization and its impact on reflectance as examined in nature, and ultimately from space-based platforms.

Acknowledgements

We thank Craig S. T. Daughtry, Andrew Russ and James E. McMurtrey (retired) of USDA, Milton Hom (SSAI) for ASD calibration, Maryn Butcher (formerly, SSAI) for assistance with measurements, and Diane Wickland (NASA HQ) for funding support.

References

- ALONSO, L., GOMEZ, L., AMOROS, J., VILA, J., GUANTER, L., CALPE, J. and MORENO, J., 2007, Sensitivity analysis of the FLD method for the measurement of chlorophyll fluorescence using a field spectroradiometer. In *3rd International Workshop on Remote Sensing of Vegetation Fluorescence*, 7–9 February 2007, Florence, Italy, CD-ROM.
- CAMPBELL, P.K.E., MIDDLETON, E.M., CORP, L.A. and KIM, M.S., 2008, Contribution of chlorophyll fluorescence to the apparent reflectance of vegetation. *Science of the Total Environment* (Special Issue of the 2006 Biogeomon Conference), DOI 10.1016/j.scitotenv.2007.11.004, in press.
- CAMPBELL, P.K.E., MIDDLETON, E.M., CORP, L.A., MCMURTREY, J.E., III., KIM, M.S., CHAPPELLE, E.W. and BUTCHER, L.M., 2002, Chlorophyll fluorescence and apparent red/near-infrared reflectance of corn foliage subjected to nitrogen deficiency. In *Proceedings, International Geoscience and Remote Sensing Symposium (IGARSS'02)*, 23–27 June, Toronto, Canada, CD-ROM.
- CORP, L.A., MCMURTREY, J.E., MIDDLETON, E.M., MULCHI, C.L., CHAPPELLE, E.W. and DAUGHTRY, C.S.T., 2003, Fluorescence sensing systems: in vivo detection of biophysical variations in field corn due to nitrogen supply. *Remote Sensing of Environment*, **86**, pp. 470–479.
- CORP, L.A., MIDDLETON, E.M., DAUGHTRY, C.S.T. and CAMPBELL, P.K.E., 2006a, Solar induced fluorescence and reflectance sensing techniques for monitoring

- nitrogen utilization in corn. In *Proceedings, International Geoscience and Remote Sensing Symposium (IGARSS 2006)*, 1–5 August 2006, Denver, CO, CD-ROM.
- CORP, L.A., MIDDLETON, E.M., DAUGHTRY, C.S.T., CAMPBELL, P.K.E., HUENNRICH, K.F. and CHENG, Y.B., 2008, Impact of spectral resolution on solar induced fluorescence and reflectance indices for monitoring vegetation. In *Proceedings, International Geoscience and Remote Sensing Symposium*, 6–11 July, Boston, MA, CD-ROM.
- CORP, L.A., MIDDLETON, E.M., MCMURTREY, J.E., CAMPBELL, P.K.E. and BUTCHER, L.M., 2006b, Fluorescence sensing techniques for vegetation assessment. *Applied Optics*, **45**, pp. 1023–1033.
- DOBROWSKI, S.Z., PUSHNIK, J.C., ZARCO-TEJADA, P.J. and USTIN, S.L., 2005, Simple reflectance indices track heat and water stress-induced changes in steady-state chlorophyll fluorescence at the canopy level. *Remote Sensing of Environment*, **97**, pp. 403–414.
- GUANTER, L., ALONSO, L., GOMEZ-CHOVA, L., AMOROS-LOPEZ, J., VILA, J. and MORENO, J., 2007, Estimation of solar-induced vegetation fluorescence from space measurements. *Geophysical Research Letters*, **34**, pp. L08401.
- LIU, L., ZHANG, Y., WANG, J. and ZHAO, C., 2005, Detecting solar-induced chlorophyll fluorescence from field radiance spectra based on Fraunhofer line principle. *IEEE Transactions of Geoscience and Remote Sensing*, **43**, pp. 827–832.
- LOUIS, J., OUNIS, A., DUCRUET, J.-M., EVAIN, S., LAURILA, T., THUM, T., AURELA, M., WINGSLE, G., ALONSO, L., PEDROS, R. and MOYA, I., 2005, Remote sensing of sunlight-induced chlorophyll fluorescence and reflectance of Scots pine in the boreal forest during spring recovery. *Remote Sensing of Environment*, **96**, pp. 37–48.
- MERONI, M. and COLOMBO, R., 2006, Leaf level detection of solar induced chlorophyll fluorescence by means of a subnanometer resolution spectroradiometer. *Remote Sensing of Environment*, **103**, pp. 438–448.
- MIDDLETON, E.M., CORP, L.A., DAUGHTRY, C.S.T. and CAMPBELL, P.K.E., 2006, Chlorophyll fluorescence emissions of vegetation canopies from high resolution field reflectance spectra. In *Proceedings, International Geoscience and Remote Sensing Symposium (IGARSS 2006)*, 1–5 August 2006, Denver, CO, CD-ROM.
- MIDDLETON, E.M., CORP, L.A., DAUGHTRY, C.S.T., CAMPBELL, P.K.E. and BUTCHER, M.L., 2005, Deriving chlorophyll fluorescence emissions of vegetation canopies from high resolution field reflectance spectra. In *SPIE, Optical Sensors and Sensing Systems for Natural Resources and Food Quality*, 23–27 October 2005, Boston, MA, Conference SA 104.
- MORENO, J., 2005, FLEX-Fluorescence Explorer: a mission concept proposal in response to the European Space Agency's Earth Explorer Core Missions 2005 concept call, submitted August 2005 [one of six concepts selected in 2006 for pre-Phase A studies. Available online at http://en.wikipedia.org/wiki/FLEX_mission].
- MOYA, I., CAMENEN, L., EVAIN, S., GOULAS, Y., CEROVIC, Z.G., LATOUCHE, G., FLEXAS, J. and OUNIS, A., 2004, A new instrument for passive remote sensing. 1. Measurements of sunlight-induced chlorophyll fluorescence. *Remote Sensing of Environment*, **91**, pp. 186–197.
- MOYA, I., CARTELAT, A., CEROVIC, Z.G., DUCRUET, J.-M., EVAIN, S., FLEXAS, J., GOULAS, Y., LOUIS, J., MEYER, S., MOISE, N. and OUNIS, A., 2003, Possible approaches to remote sensing of photosynthetic activity. In *Proceedings, International Geoscience and Remote Sensing Symposium (IGARSS'03)*, 21–25 July, Toulouse, France, CD-ROM.
- PEDRÓS, R., JACQUEMOUD, S., GOULAS, Y., LOUIS, J. and MOYA, I., 2005, A new leaf fluorescence model. In *2nd International Workshop on Remote Sensing of Vegetation Fluorescence*, 17–19 November 2004, Montreal, Canada, CD-ROM.
- PLASCYK, J., 1975, The MKII Fraunhofer line discriminator (FLD-II) for airborne and orbital remote sensing of solar-stimulated luminescence. *Optical Engineering*, **14**, pp. 339–346.

- ROSEMA, A., SNEL, J.F.H., ZAHN, H., BUURMEIJER, W.F. and VAN HOVE, L.W.A., 1998, The relation between laser-induced chlorophyll fluorescence and photosynthesis. *Remote Sensing of Environment*, **65**, pp. 143–154.
- THEISEN, A.F., 2000, A passive method for detecting vegetation stress from orbit: chlorophyll fluorescence from Fraunhofer lines. In *Proceedings, RS2000, Soil Science Society of America (SSSA)*, 22–25 October, Corpus Christi, TX, USA, CD-ROM.
- VERHOEF, W., 1984, Light scattering by leaf layers with application to canopy reflectance modelling: the SAIL model. *Remote Sensing of Environment*, **16**, pp. 125–141.
- VERHOEF, W., 1998, Theory of radiative transfer models applied in optical remote sensing of vegetation canopies. PhD thesis, Wageningen Agricultural University.
- VERHOEF, W., 2005, FluorMOD: extension of SAIL to model solar-induced canopy fluorescence spectra. In *2nd International Workshop on Remote Sensing of Vegetation Fluorescence*, 17–19 November 2004, Montreal, Canada, CD-ROM.
- WELLBURN, A., 1994, The spectral determination of chlorophylls a and b, as well as total carotenoids using various solvents with spectrophotometers of different resolution. *Journal of Plant Physiology*, **144**, pp. 307–313.
- ZARCO-TEJADA, P.J., MILLER, J.R., MOHAMMED, G.H. and NOLAND, T.L., 2000, Chlorophyll fluorescence effects on vegetation apparent reflectance: I. Leaf-level measurements and model simulation. *Remote Sensing of Environment*, **74**, pp. 582–595.
- ZARCO-TEJADA, P.J., MILLER, J.R., PEDRÓS, R., VERHOEF, W. and BERGER, M., 2004a, FluorMODgui: a graphic user interface for the spectral simulation of leaf and canopy fluorescence effects. In *2nd International Workshop on Remote Sensing of Vegetation Fluorescence*, 17–19 November, Montreal, Canada, CD-ROM.
- ZARCO-TEJADA, P.J., PÉREZ-PRIEGO, O., SEPULCRE-CANTÓ, G., MILLER, J.R. and FERERES, E., 2004b, Chlorophyll fluorescence detection with a high-spectral resolution spectrometer through in-filling of the O₂-A band as a function of water stress in olive trees. In *2nd International Workshop on Remote Sensing of Vegetation Fluorescence*, 17–19 November, Montreal, Canada, CD-ROM.